PHYS 5047 INTRODUCTION TO COMPUTATIONAL METHODS

Term Project I Report

Aysu Ece SARICAOGLU

519960

Department of Physics, Washington University in St. Louis,

University City, 63130, St. Louis, USA

Project 1: Ray-tracing a Black Hole Image

1 Introduction

In this project, the geodesic equation for photons was numerically solved to create a ray-tracing image of a black hole. Two test cases for the photon trajectories were simulated in the distorted space-time. Finally, the accretion disk was simulated around the event horizon with various initial parameters.

2 Methods

With `C++`, the metric equations given [1] were evaluated to calculate the trajectories, utilizing the numerical ODE solver *RK45 Dormand-Prince* and *RK4* methods. These methods were chosen for both their high accuracy and efficiency. The metric equations are evaluated by the `class boyer_lindquist_metric` in the header file `project.h`. For the first test, `class rk4_adaptive_sol` was used in the header file `rk4_adaptive.h`. For the second test and the final ray-tracing task, `class rk45_dormand_prince` was used in the header file `rk45.h`. Note that both solver methods were acquired from the previous homework solutions.

For each task, separate `.cpp` files were scripted, and their outputs are saved in separate `.csv` files for each case included. `Python` scripts were used to plot the photon trajectories and the final step image with `matplotlib` library.

- **Task I)** Script : `project_1.cpp`. Output(s) : `output1-a.csv`, `output1-b.csv`, Plotting : `plots_1.py`.
- **Task II)** Script : `project_2.cpp`. Output(s) : `output2A.csv`, `output2B.csv`, `output2C.csv`, `output2D.csv`, `output2E.csv`. Plotting : `plots_2.py`.
- **Task III)** Script : `project_3.cpp`, Output(s) : `output_raytracing1-a.csv`, `output_raytracing1-b.csv`, `output_raytracing2-a.csv`, `output_raytracing2-b.csv`, `output_raytracing3-a.csv`, `output_raytracing3-b.csv`. Plotting : `plots_3.py`

.

Although *RK45 Dormand-Prince* and *RK4* methods were useful tools for the simulation, they may misbehave around possible singularities. Such behavior is suspected around $x = 0$, as a possible cause of the thin, black lines on the ray tracing images of Task III.

3 Task I: Einstein Ring in Schwarzschild Spacetime

The photon trajectories were simulated for two different sets of parameters around a non-rotating black hole, with spin parameter a = 0.

3.1 Case I : $r_{obs} = 10$M, $\xi = 0.48857874$

The photon trajectory for the first set of parameters is shown in Figure 1 with the stop condition $\phi = 2\pi$. The final position of the photon slightly deviates from the r_{obs}, with an interpolation value of 0.1116063691358088. This error might be a result of a minor instability of the trajectory for the given parameters.

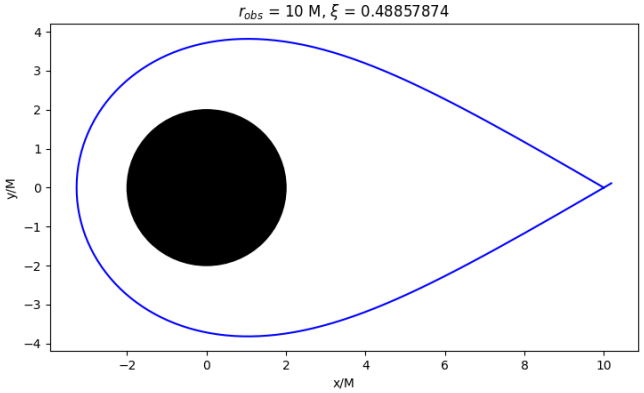

Figure 1: Photon trajectory for $\phi = 2\pi$. The photon goes around the black hole exactly once and comes back.

3.2 Case II : $r_{obs} = 20$M, $\xi = 0.24904964$

The photon trajectory for the second set of parameters is shown in Figure 2 with the stop condition $\phi = 4\pi$. The final position of the photon is the r_{obs}, with an interpolation value of 0.0. Therefore, the error in the first case is unlikely to be a result of numerical integration. Otherwise, this case would have a higher numerical error accumulated during the integration over a longer duration.

4 Task II : Unstable Spherical Photon Orbits in Kerr Spacetime

Unstable spherical photon orbits were simulated around a maximally spinning black hole, with a = 1. These orbits and their initial conditions for r, u_θ, u_ϕ are given in Table 1 [1] of the project description, and simulated

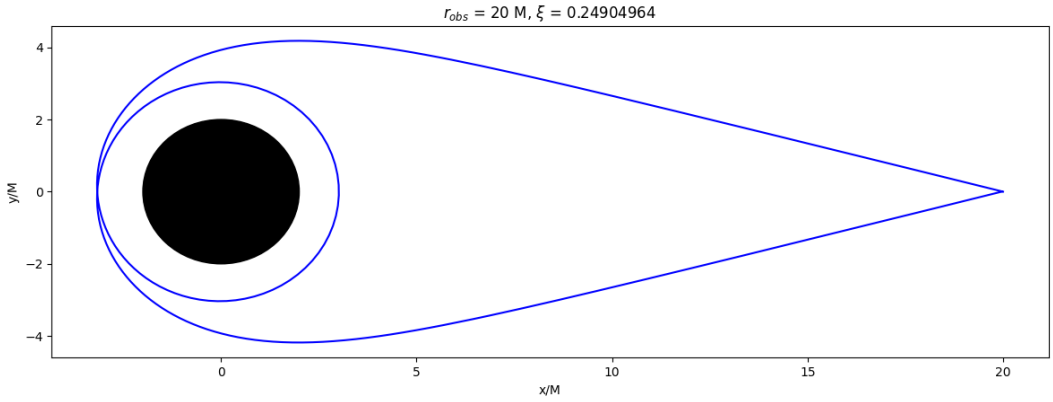

Figure 2: Photon trajectory for $\phi = 4\pi$. The photon goes around the black hole twice and comes back.

orbits are shown in Figure 3. Figure 4 shows the duration for each orbit to become unstable. While Orbit D has the highest instability, the longest stable duration is observed for Orbit A.

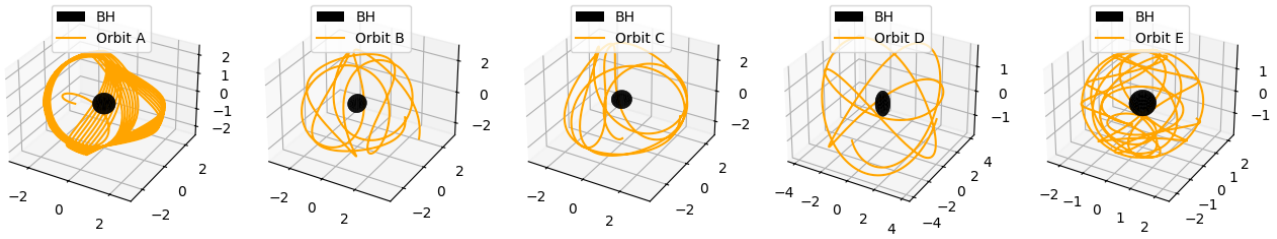

Figure 3: Spherical orbits A, B, C, D, and E around a Kerr black hole. The unstable orbits were plotted with the stop condition $|r_{final} - r_{initial}| \geq 0.9$, to stop the numerical integration when the photon falls into the black hole or escapes from the orbit.

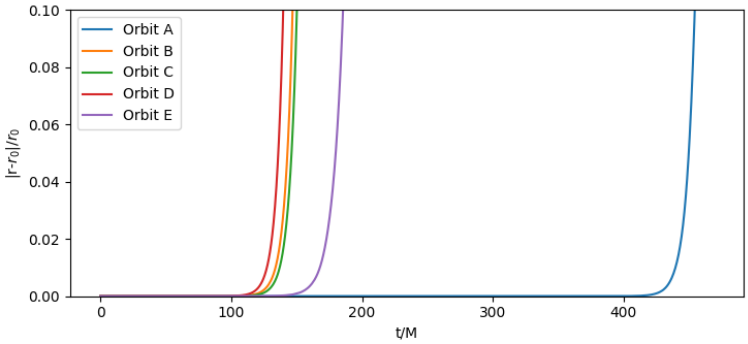

Figure 4: The error evolution of r for spherical orbits A, B, C, D, and E.

5 Task III: Creating a Black Hole Image

For the final step, ray-tracing images for black holes with various combinations of inclination angles θ_0 and spin parameters a were constructed. At the distance $D = 500$, a screen of dimensions 50×50 in x and y with step sizes $dx = 0.1$, $dy = 0.1$ for Case I-a and $dx = 0.25$, $dy = 0.25$ for Case I-b, Case II and Case III were used.

5.1 Case I : $\theta_0 = 85°$

This is the view that the black hole is observed almost edge-on to the accretion disk. Important features such as the photon ring around the event horizon shadow, bending of the back side of the accretion disk towards the upside due to the gravitational lensing, and the redshift of the light for the photons moving away from the observer.

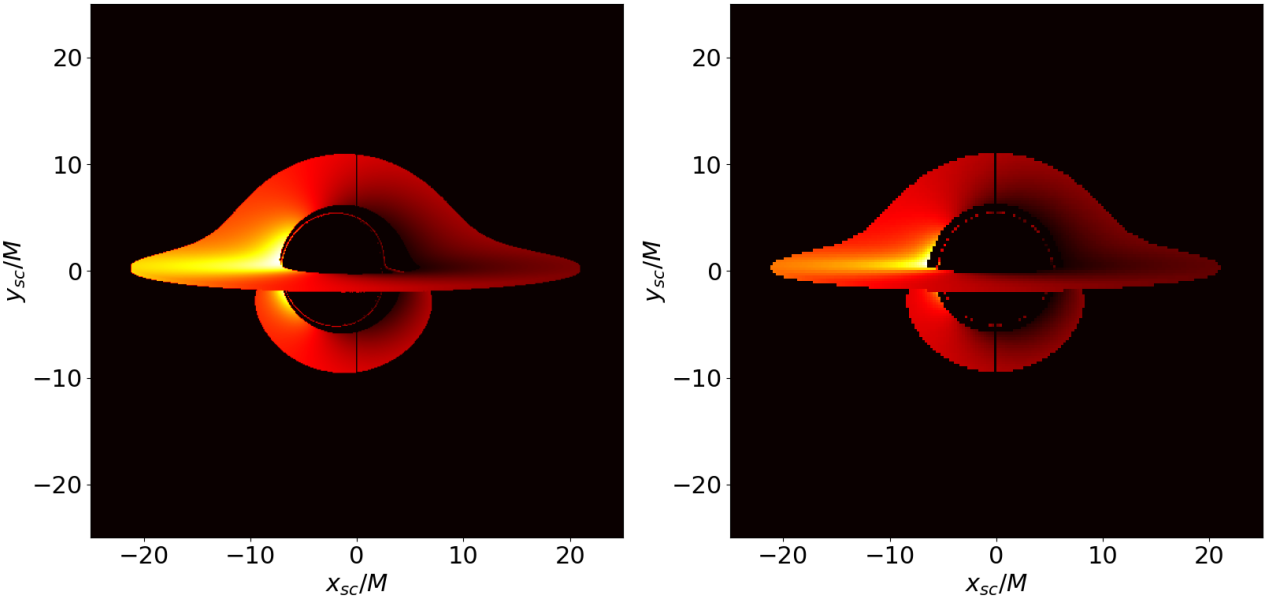

Figure 5: Ray tracing image of a maximally (a) rotating Kerr black hole with $a = 0.99$ (left) and (b) a non-rotating black hole with $a = 0$ (right) for $\theta_0 = 85°$.

Comparing the rotating and non-rotating cases in Figure 5, it can be seen that the Doppler effect is stronger for the Kerr black hole. Moreover, the photon ring is shifted towards $-x$ direction for the rotating case while the no-rotating case has the photon ring symmetric around the origin.

5.2 Case II : $\theta_0 = 5°$

This view observes the black hole almost perpendicular to the accretion disk plane, from the north pole of the black hole. Therefore, the accretion disk is completely visible and uniform, without any effect of the gravitational lensing.

In Figure 6, the Doppler effect is also observed near to symmetric around the disk for both rotating and non-rotating cases. The completely symmetric case was predicted for $\theta_0 = 0°$ and intended for simulation, however, the compiling time for the program was not feasible.

5.3 Case III : $\theta_0 = 45°$

This view angle shares features with both of the previous cases. The Doppler effect is observable as in the first case, however, the effects of gravitational lensing are still absent similar to the second case.

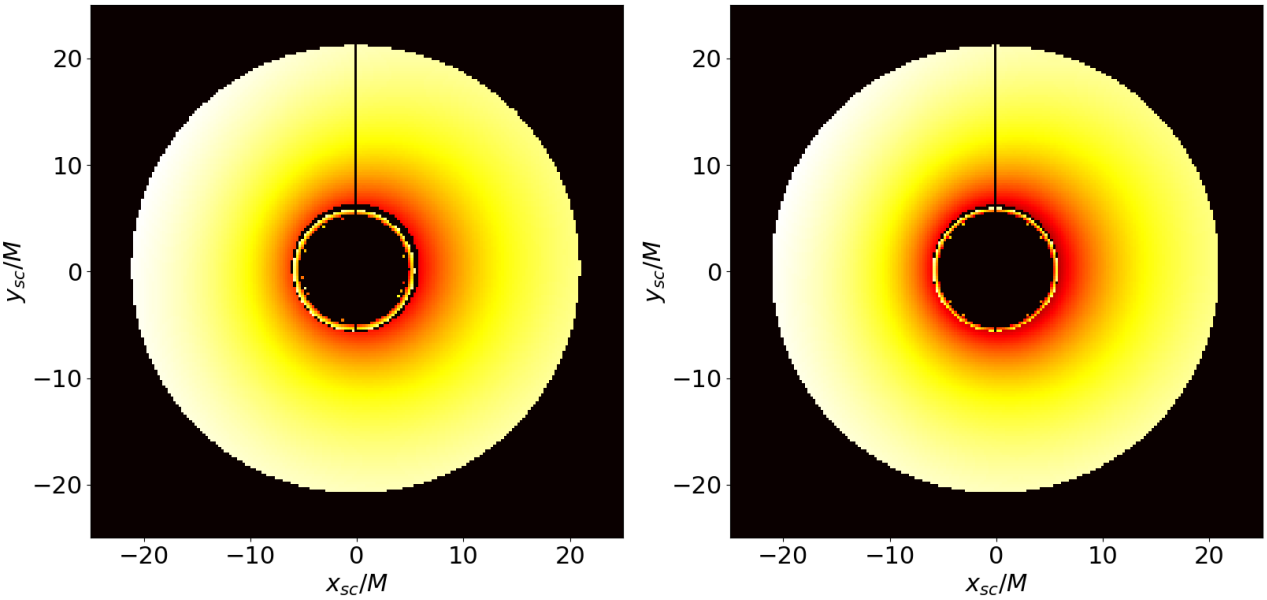

Figure 6: Ray tracing image of a maximally (a) rotating Kerr black hole with $a = 0.99$ (left) and (b) a non-rotating black hole with $a = 0$ (right) for $\theta_0 = 5°$.

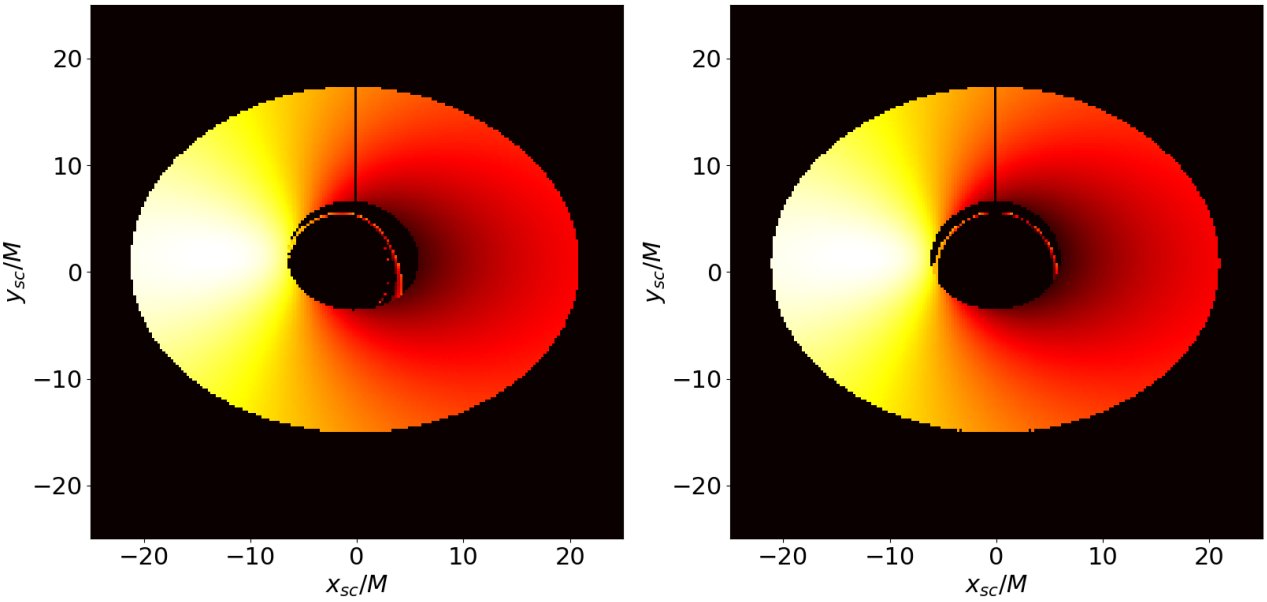

Figure 7: Ray tracing image of a maximally (a) rotating Kerr black hole with $a = 0.99$ (left) and (b) a non-rotating black hole with $a = 0$ (right) for $\theta_0 = 45°$.

The effect of rotation can be observed by the difference in the photon sphere orientations from Figure 7.

References

[1] A. Chen. "Project 1: Raytracing a black hole image," Washington University in St. Louis. (2023).